SUPPORTING MATERIALS

ST2 as checkpoint target for colorectal cancer immunotherapy

Kevin Van der Jeught[1], Yifan Sun[1], Yuanzhang Fang[1], Zhuolong Zhou[1], Hua Jiang[2], Tao Yu[1], Jinfeng Yang[2], Malgorzata Maria Kamocka[3], Kaman So[4], Yujing Li[1], Haniyeh Eyvani[1], George E. Sandusky[5], Michael Frieden[1], Harald Braun[6,7], Rudi Beyaert[6,7], Xiaoming He[8,9] , Xinna Zhang[1,10], Chi Zhang[1,4,10], Sophie Paczesny[2,10*], Xiongbin Lu[1,10*]

[1]Department of Medical and Molecular Genetics, Indiana University School of Medicine, Indianapolis, IN, USA; [2]Department of Pediatrics, Indiana University School of Medicine, Indianapolis, IN, USA; [3]Department of Medicine, Division of Nephrology, Indiana University School of Medicine, Indianapolis, IN, USA; [4]Center for Computational Biology and Bioinformatics, Indiana University School of Medicine, Indianapolis, IN, USA; [5]Department of Pathology and Laboratory Medicine, Indiana University School of Medicine, Indianapolis, IN, USA; [6]VIB Center for Inflammation Research, Ghent, Belgium; [7]Department of Biomedical Molecular Biology, Ghent University, Ghent, Belgium; [8]Fischell Department of Bioengineering, University of Maryland, College Park, MD, USA; [9]Marlene and Stewart Greenebaum Comprehensive Cancer Centre, University of Maryland, Baltimore, MD, USA; [10]Melvin and Bren Simon Cancer Center, Indiana University School of Medicine, Indianapolis, IN, USA

[*]Corresponding authors:

[*]Sophie Paczesny, MD, PhD

Nora Letzter Professor of Pediatrics

Indiana University School of Medicine

Professor, Microbiology & Immunology

Melvin and Bren Simon Cancer Center

Wells Center for Pediatric Research

1044 W Walnut Street, R4 425

Indianapolis, IN 46202

317-278-5487 (office)

sophpacz@iu.edu

*Xiongbin Lu, PhD

Vera Bradley Foundation Chair in Breast Cancer Innovation

Strategic Research Initiative Distinguished Investigator

Indiana University Melvin and Bren Simon Cancer Center

Professor, Medical and Molecular Genetics

Indiana University School of Medicine

980 W Walnut St, R3.C218D

Indianapolis, IN 46202

317-274-4398 (office)

xiolu@iu.edu

SUPPORTING SUPPLEMENTARY FIGURE LEGENDS

Supplementary Figure 1. Computational gene correlation analysis of T cell anti-tumor immunity. Violin box plots for the correlation of *IL1RL1* expression with the normalized expression of GNLY, CD8B and IFNG genes. Data analysis was conducted using the ICTD algorithm on 93 (*IL1RL1* High, 53 patients; *IL1RL1* Low, 40 patients) biologically independent colorectal cancer patients from the TCGA database. Significance was determined by two-tailed unpaired *t* test.

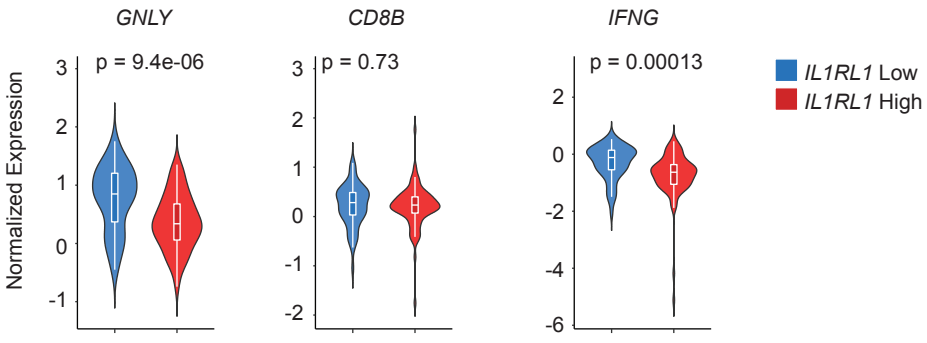
GNLY
CD8B
IFNG
p = 9.4e-06
p = 0.73
p = 0.00013
Normalized Expression
3
2
1
0
-1
-2
-4
-6
IL1RL1 Low
IL1RL1 High

Supplementary Figure 2. Tumor growth of MC38 and CT26 tumors in *WT* and *ST2*$^{-/-}$ mice. (**A**) Tumor growth curve of MC38 (left panel) and CT26 (right panel) in *WT* and *ST2*$^{-/-}$ mice (C57BL/6 *WT* n=8*;* C57BL/6 *ST2*$^{-/-}$ n=7*;* BALB/C *WT* n=8; BALB/C *ST2*$^{-/-}$ n=9; Data displayed as mean + SEM). The data represents one tumor growth experiments out of at least 3 independent experiments. (**B**) Individual spaghetti plots from both male and female mice of the tumor growth shown in *figure 2B*. Significance was determined by two-way ANOVA (**A**).

A

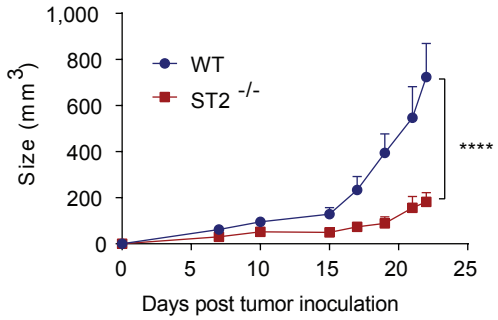
1,000
800
600
400
200
0
Size (mm3)
WT
ST2 -/-
****
0
5
10
15
20
25
Days post tumor inoculation

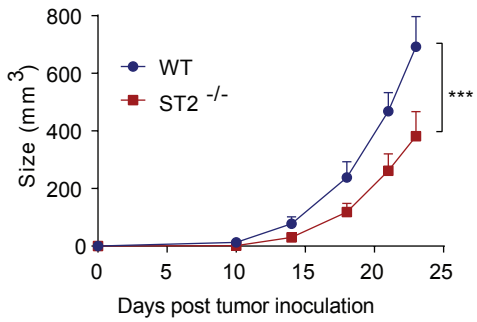
800
600
400
200
0
Size (mm3)
WT
ST2 -/-
***
0
5
10
15
20
25
Days post tumor inoculation

B

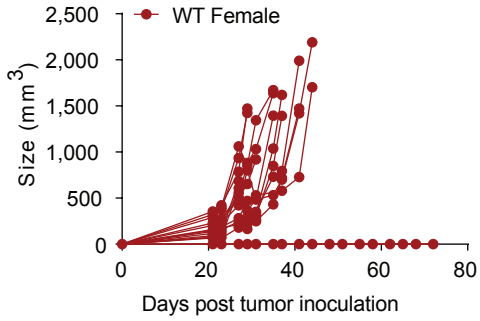
2,500
2,000
1,500
1,000
500
0
Size (mm3)
WT Female
0
20
40
60
80
Days post tumor inoculation

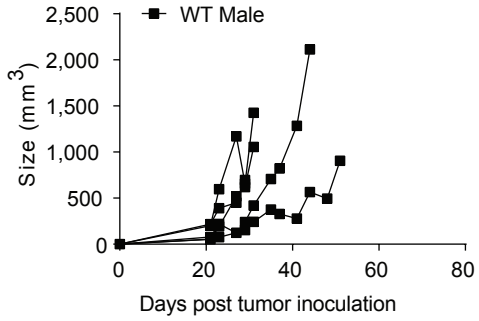
2,500
2,000
1,500
1,000
500
0
Size (mm3)
WT Male
0
20
40
60
80
Days post tumor inoculation

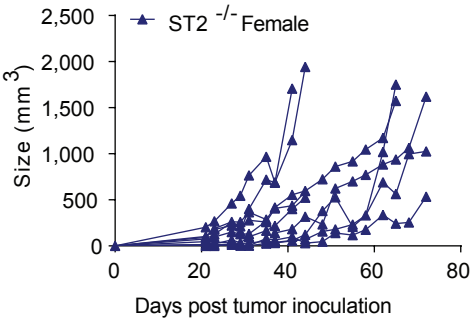
2,500
2,000
1,500
1,000
500
0
Size (mm3)
ST2 -/- Female
0
20
40
60
80
Days post tumor inoculation

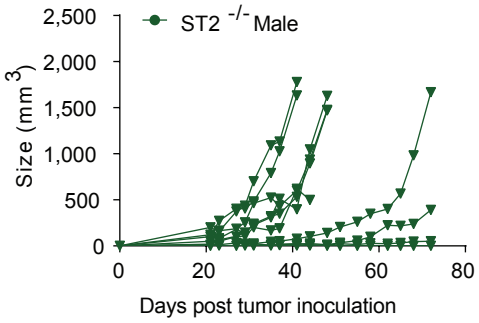
2,500
2,000
1,500
1,000
500
0
Size (mm3)
ST2 -/- Male
0
20
40
60
80
Days post tumor inoculation

Supplementary Figure 3. CyTOF phenotyping of *WT* and *ST2*$^{-/-}$ mice harboring MC38 tumors. (**A, B**) Mass cytometry immune cell analysis on MC38 injected tumor cells in *WT* and *ST2*$^{-/-}$ mice (*n*=5 mice per group). (**A**) t-SNE plot of tumor infiltrating lymphocytes after running SPADE on viSNE. The plot shows the clustering on the tSNE1 and tSNE2 axis. (**B**) Normalized intensities on t-SNE plot of immune cells displaying the indicated channel expression levels.

A

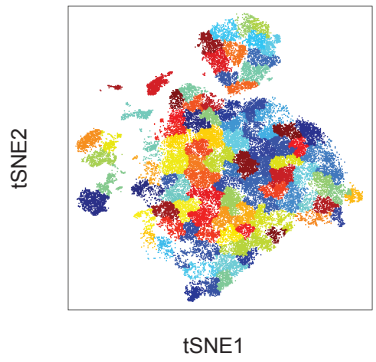
tSNE2
tSNE1

B

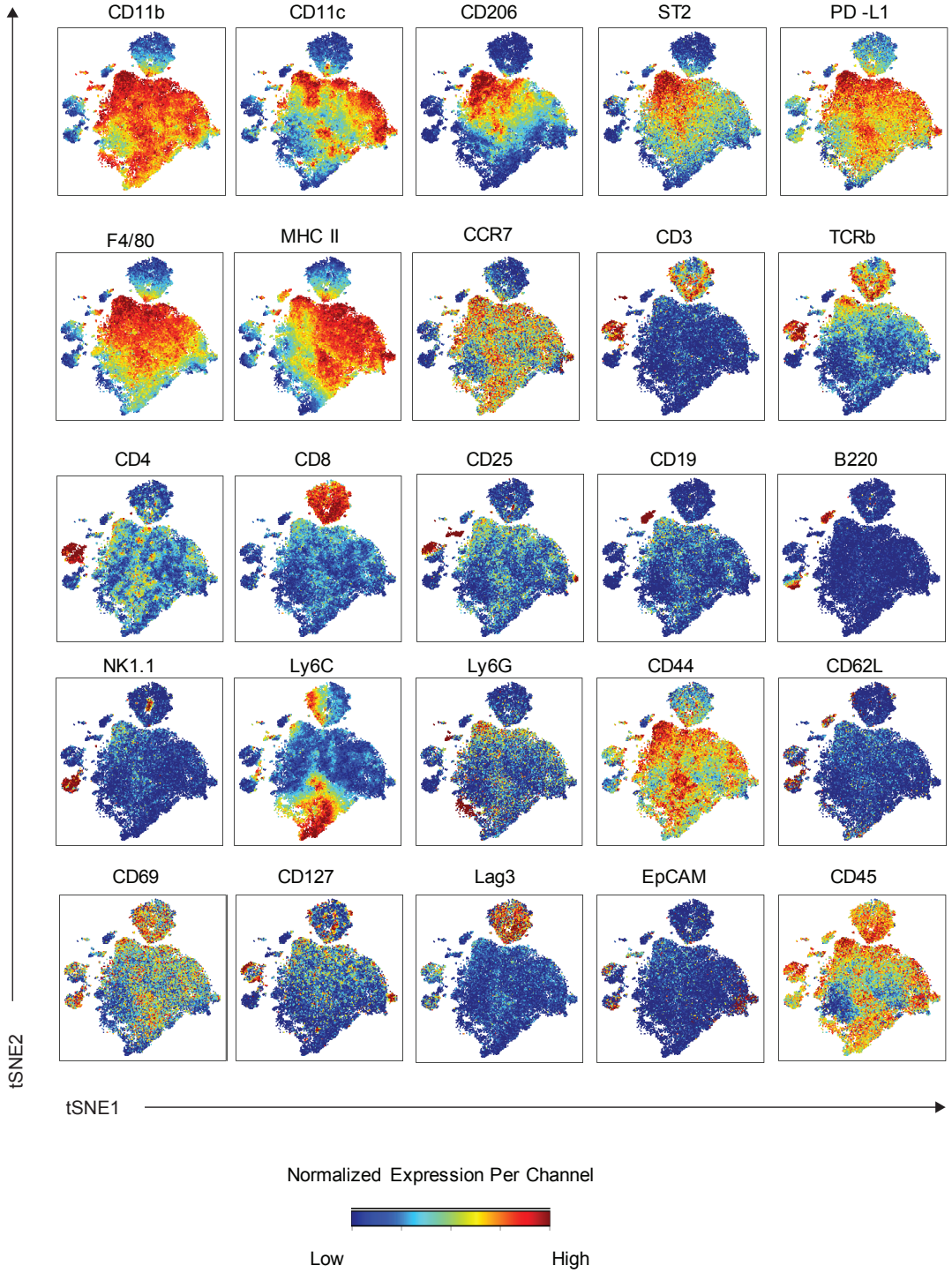
CD11b
CD11c
CD206
ST2
PD -L1
F4/80
MHC II
CCR7
CD3
TCRb
CD4
CD8
CD25
CD19
B220
NK1.1
Ly6C
Ly6G
CD44
CD62L
CD69
CD127
Lag3
EpCAM
CD45
tSNE2
tSNE1
Normalized Expression Per Channel
Low
High

Supplementary Figure 4. Validation of CD8$^+$ T cell depletion. (**A**) Flow cytometry gating strategy to monitor CD8$^+$ T-cell depletion from the mouse blood. (**B**) Representative flow cytometry plots from *WT* and *ST2*$^{-/-}$ mice upon treatment with the isotype or anti-CD8 antibody. (**C**) Quantification of the CD8$^+$ T-cell depletion from *WT* and *ST2*$^{-/-}$ mice upon treatment with the isotype or anti-CD8 antibody. (WT isotype, *n*=4; ST2$^{-/-}$ isotype, *n*=5; WT anti-CD8, *n*=4; ST2$^{-/-}$ anti-CD8, *n*=5; Data displayed as mean ± SD). Significance was determined by one-way ANOVA (**C**).

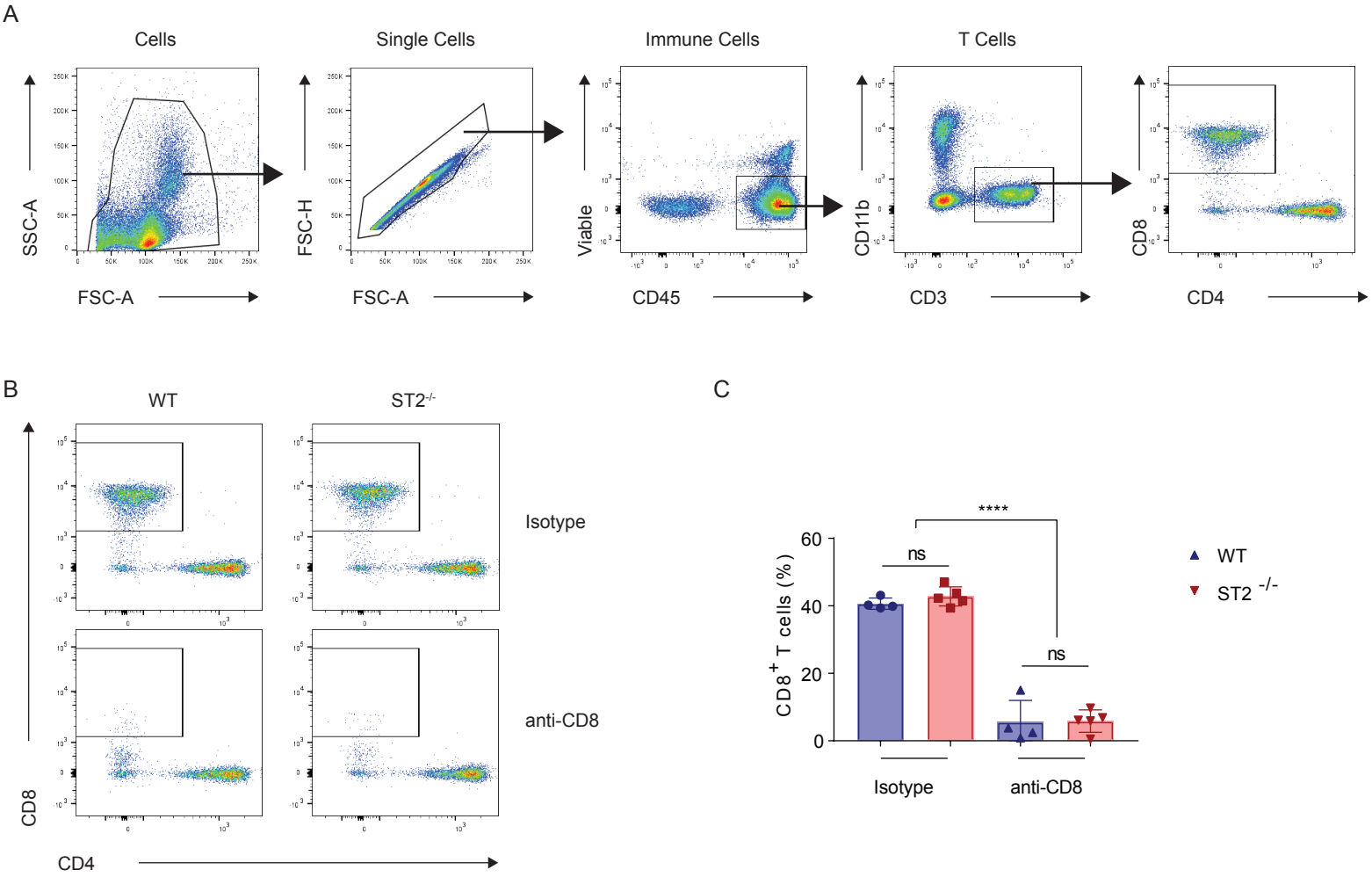
A
Cells
Single Cells
Immune Cells
T Cells
SSC-A
FSC-A
FSC-H
FSC-A
Viable
CD45
CD11b
CD3
CD8
CD4
B
WT
ST2-/-
Isotype
anti-CD8
CD8
CD4
C
****
ns
ns
60
40
20
0
CD8+ T cells (%)
WT
ST2 -/-
Isotype
anti-CD8

Supplementary Figure 5. Gating Strategy ST2 expression in the CT26 Tumor Microenvironment. (**A**) Gating strategy to assess viable immune cells in the CT26 TME. (**B**) Gating strategy to define the immune cell subtypes.

A

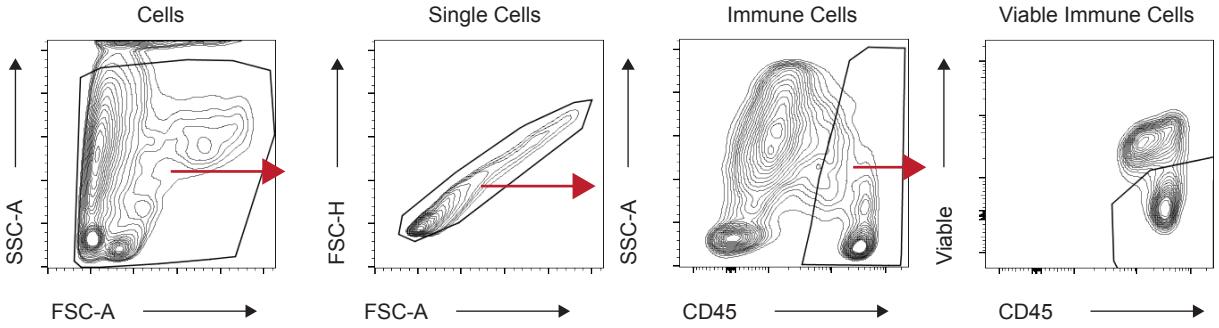
Cells
SSC-A
FSC-A
Single Cells
FSC-H
FSC-A
SSC-A
Immune Cells
CD45
Viable
Viable Immune Cells
CD45

B

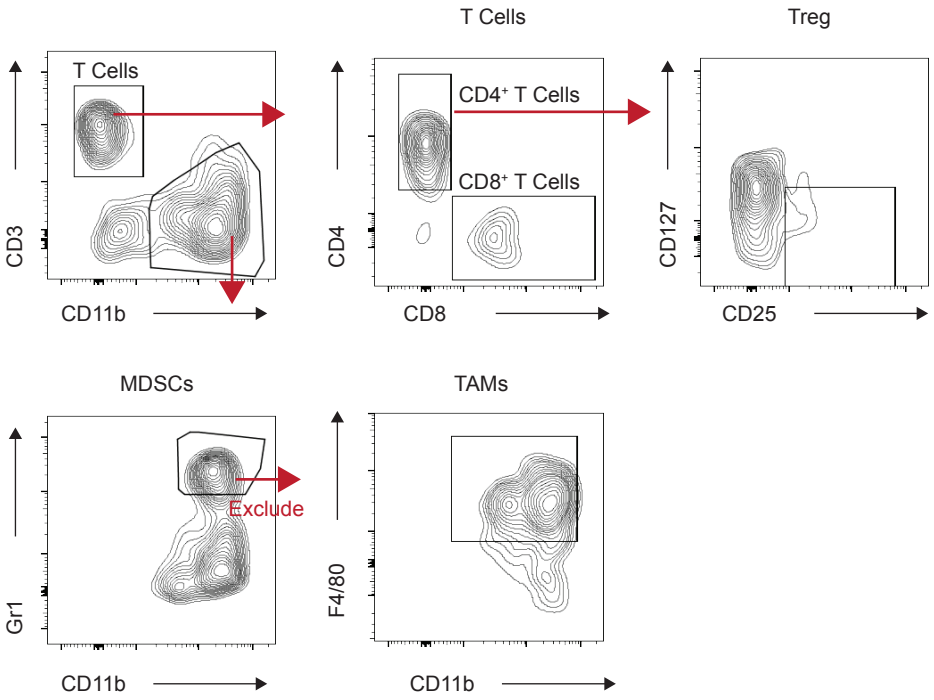
T Cells
CD3
CD11b
T Cells
CD4⁺ T Cells
CD8⁺ T Cells
CD4
CD8
Treg
CD127
CD25
MDSCs
Exclude
Gr1
CD11b
TAMs
F4/80
CD11b

Supplementary Figure 6. Orthotopic mouse colorectal cancer model. (A) Representative H&E staining of orthotopic cecal wall tumors. (B) Representative confocal microscopy images from at 20x magnification stained with the indicated markers on orthotopic cecal wall tumor of injected MC38 cells (Tumor) and from the healthy cecal wall (Healthy). Scale bar represents 50 μm.

A

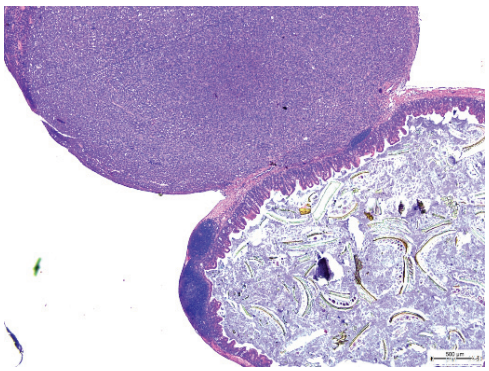

B

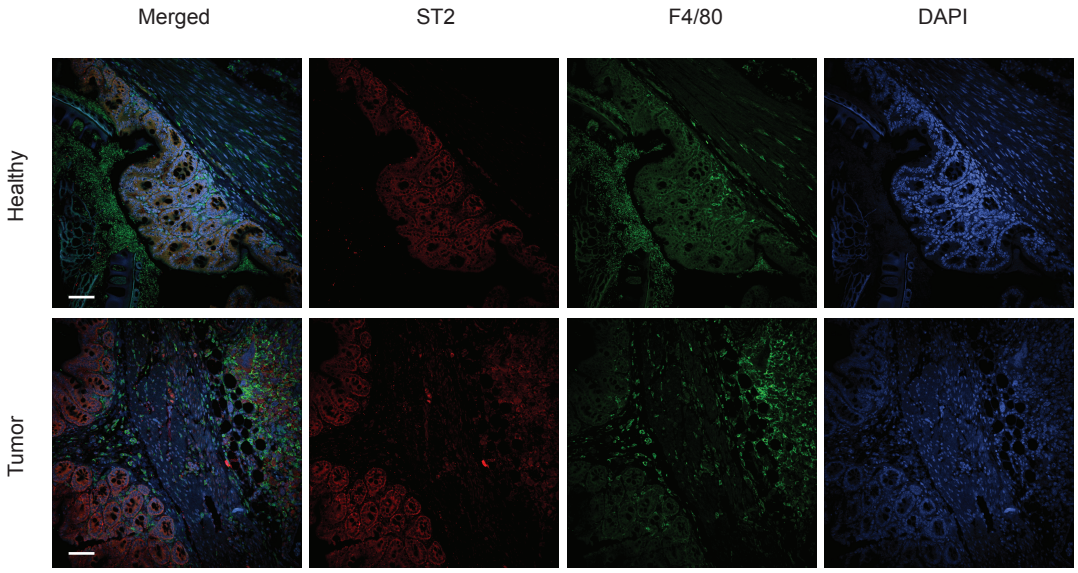

Supplementary Figure 7. Kinetic analysis of ST2^{+}TAMs in MC38 tumors. Flow cytometry analysis of ST2^{+}TAMs and ST2^{-}TAMs from MC38 tumors at the indicated time point (*n*=5; Data displayed as mean ± SD). Significance was determined by two-tailed unpaired *t* test.

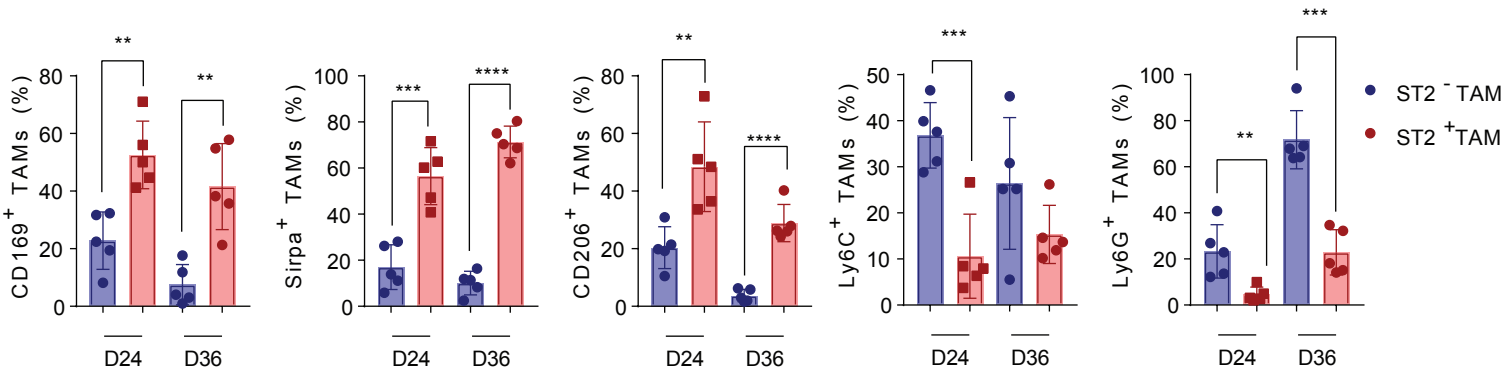
CD169+ TAMs (%)
Sirpa+ TAMs (%)
CD206+ TAMs (%)
Ly6C+ TAMs (%)
Ly6G+ TAMs (%)
D24
D36
ST2 - TAM
ST2 + TAM

Supplementary Figure 8. Schematic representation of the macrophage suppression assay and gating of T cells. (**A**) Tumors are processed into single cells; the macrophages are then enriched using MACS sorting and co-cultured with CFSE-labeled pan T cells isolated from naïve mice. (**B**) The inhibition of T-cell proliferation was assessed 5 days post co-culture. The proliferation of T cells was assessed using the following gating strategy. (**C**) Quantification of $CD4^+$ T-cell proliferation upon TAM co-culture (n=6; Data displayed as mean ± SEM). (**D**) Representative F4/80 stained tumor immunohistochemistry images from control and anti-CSF1R treated mice. Scale bar represents 50 μm. Significance was determined by two-tailed unpaired *t* test (**C**).

A

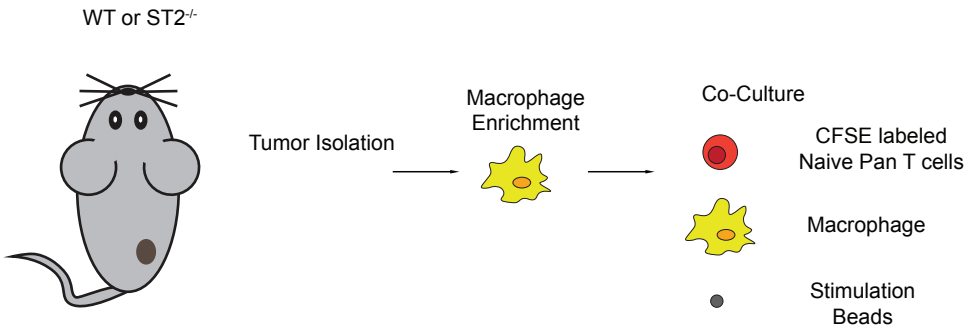
WT or ST2-/-
Tumor Isolation
Macrophage Enrichment
Co-Culture
CFSE labeled Naive Pan T cells
Macrophage
Stimulation Beads

B

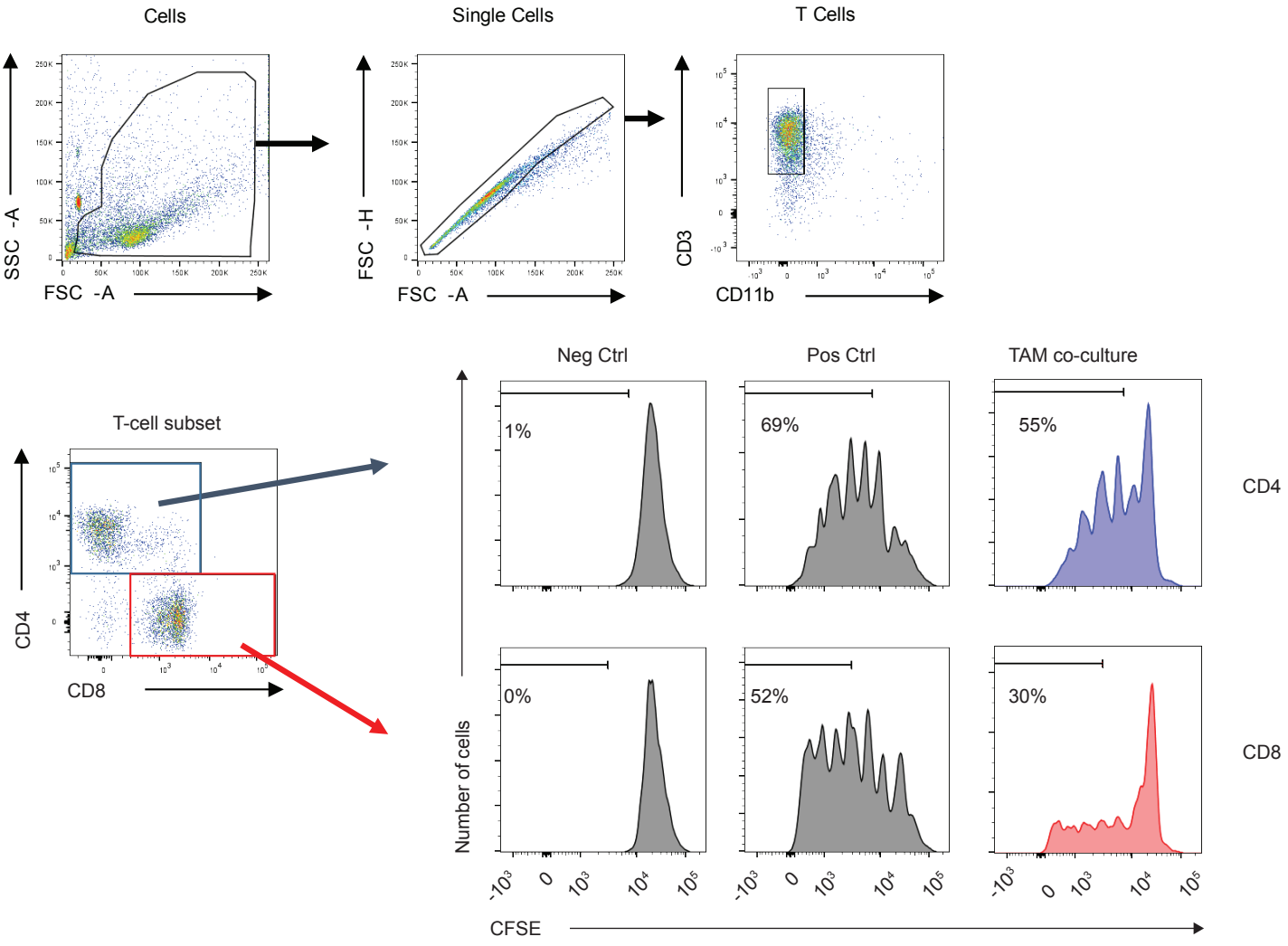
Cells
Single Cells
T Cells
SSC -A
FSC -A
FSC -H
FSC -A
CD3
CD11b
T-cell subset
CD4
CD8
Neg Ctrl
Pos Ctrl
TAM co-culture
1%
69%
55%
0%
52%
30%
CD4
CD8
Number of cells
CFSE

C

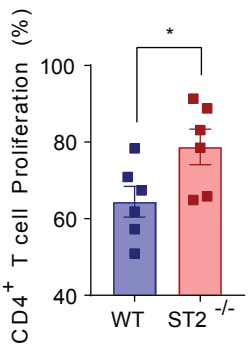
*
CD4+ T cell Proliferation (%)
100
80
60
40
WT
ST2 -/-

D

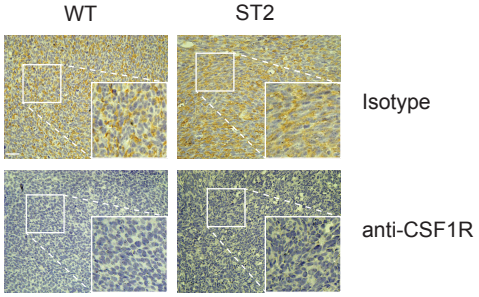
WT
ST2
Isotype
anti-CSF1R

Supplementary Figure 9. Gating Strategy for OVA-specific CD8$^+$ T cells, IL-33 enhances TAM ST2 expression. (**A**) Flow cytometry gating strategy for the quantification of blood and splenic OVA-specific CD8$^+$ T cells. (**B**) Representative confocal images from MACS F4/80 sorted macrophages from *WT* mice bearing MC38 tumors and treated or not with IL-33. Scale bar represents 10 μm.

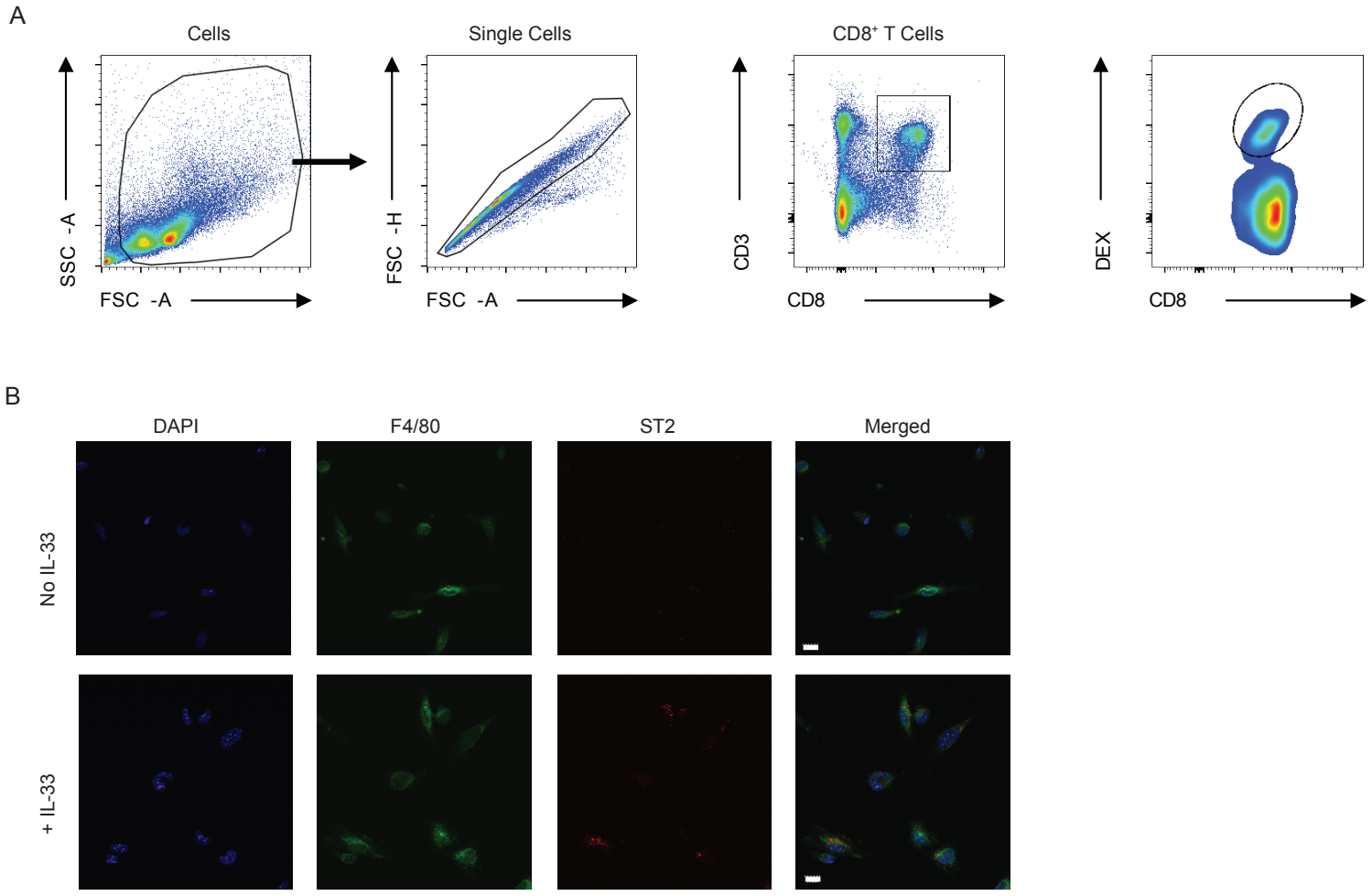
A
Cells
SSC -A
FSC -A
Single Cells
FSC -H
FSC -A
CD8⁺ T Cells
CD3
CD8
DEX
CD8
B
DAPI
F4/80
ST2
Merged
No IL-33
+ IL-33

Supplementary Figure 10. Normal phenotype of IL-33trap treated tumor-bearing mice and T-cell infiltration. (**A**) Body weight of mice treated with PBS (Control, Ctrl) or with IL-33trap (Ctrl, *n=7*, IL-33trap, *n=5*; Data displayed as mean ± SEM). (**B**) H&E pictures from the indicated organs in MC38-tumor bearing mice, treated with PBS only (Control) or IL-33trap (*n=3*). Scale bar represents: Heart (control 1x: 4 mm; control 15x: 200 μm; IL-33trap 1x: 3 mm; IL-33trap 15x: 200 μm), Kidney (control 1x: 3 mm; control 15x: 200 μm; IL-33trap 1x: 4 mm; IL-33trap 15x: 200 μm), Liver (control 1x: 4 mm; control 15x: 200 μm; IL-33trap 1x: 5 mm; IL-33trap 15x: 200 μm), Lung (control 1x: 3 mm; control 15x: 200 μm; IL-33trap 1x: 3mm; IL-33trap 15x: 200 μm), Spleen (control 1x: 3 mm; control 15x: 200 μm; IL-33trap 1x: 2mm; IL-33trap 15x: 200 μm). (**C**) Determination of the number of $CD4^+$ T cells and $CD8^+$ T cells from ctrl and IL-33trap treated mice (*n=5*; Data displayed as mean ± SD). Significance was determined by two-way ANOVA (**A**), and by two-tailed unpaired *t* test (**C**).

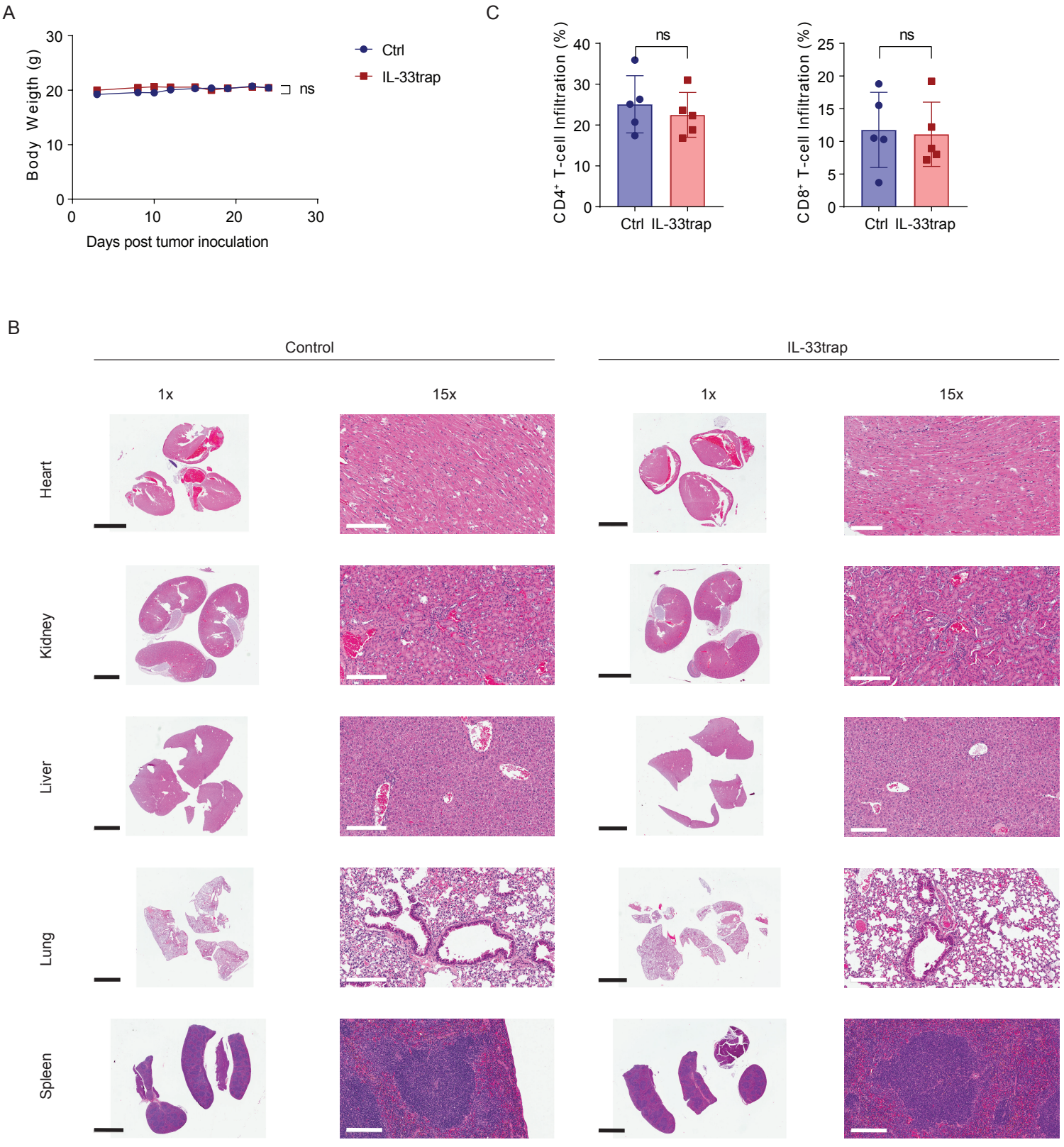
A
Body Weigth (g)
30
20
10
0
0
10
20
30
Days post tumor inoculation
ns
Ctrl
IL-33trap
C
CD4+ T-cell Infiltration (%)
40
30
20
10
0
ns
Ctrl
IL-33trap
CD8+ T-cell Infiltration (%)
25
20
15
10
5
0
ns
Ctrl
IL-33trap
B
Control
IL-33trap
1x
15x
1x
15x
Heart
Kidney
Liver
Lung
Spleen